Equating reference cell and broadband pyranometer data.

Josh Peterson[1],
Afshin Andreas[2], Aron Habte[2], Manajit Sengupta[2]

[1]Material Science Institute/University of Oregon, Eugene, Oregon, 97403 (USA)
[2]National Renewable Energy Laboratory, Golden, Colorado, 80401 (USA)

Abstract — **An adjustment algorithm has been developed for broadband Class-A pyranometers, to modify the pyranometer data such that it more closely matches that of silicon-based reference cells. The adjustment algorithm uses modeled clear-sky spectral data as one of its inputs. The adjustment also uses a reference cell angle of incidence modifier. A comparison between the pyranometer and the reference cells is performed with and without the adjustment applied. The adjustment aligns the pyranometer and reference cell data to within ±2% under clear skies when the zenith angle is less than 70°.**

Keywords— *Solar reference cells, pyranometer, spectral irradiance, spectral responsivity, incident angle modifier*

1. Introduction

Reference cells are becoming increasingly popular to monitor and evaluate the performance of photovoltaic systems in the field. Reference cells have several appealing traits that are responsible for their widespread use in industry [1]. They can be placed in the plane-of-array (POA) of the PV array. Reference cells are typically less expensive than high quality pyranometers. Reference cells are stable and have a similar spectral response to that of the PV array.

However, due to differences in the technologies between pyranometers reference cells, measurements between the two sensor types can vary considerably. Because of these differences reference cells and pyranometers typically demonstrate significant variations throughout the day and year. This makes comparisons of reference cells and pyranometers difficult.

The overarching goal of this project is to understand, characterize, and evaluate the measurements from reference cells. This goal is accomplished through the development of a reference cell model that can accurately predict the output of a reference cell under a diverse set of experimental conditions.

This study expands on previous studies in that reference cell data is compared to data from a broadband Class-A thermopile pyranometer. An adjustment algorithm is applied to the data from the pyranometer to generate a data set similar to that of a reference cell. In this way the reference cell data can be directly compared to data from a thermopile pyranometer.

This paper is organized as follows. First an introduction to the problem is given, demonstrating how reference cells and pyranometer measurements differ throughout the day. Then the adjustment algorithm used to modify the pyranometer data is outlined. Section 4 gives a description of the experimental and modeled data used in this study. In section 5 the results of the adjustment are given, demonstrating the improvement of the adjustment.

2. Introduction to the problem

The experimental data used in this study was collected at SRRL in Golden Colorado using global horizontal pyranometers and reference cells [2]. The pyranometer used in this study was a CMP22 calibrated at NREL [3]. The reference cell used in this study is a silicon mono-crystalline IMT Solar (IMT) also calibrated at NREL.

The irradiance of the two sensors is shown in the upper plot of Figure 1. The data shown here corresponds to a single clear-sky day and the calibrated responsivity values of both sensors have been applied. In the center plot the difference between the two sensors is shown. In the lower plot the percentage difference between the two sensors is shown. In all plots the horizontal axis is the solar azimuthal angle (SAA).

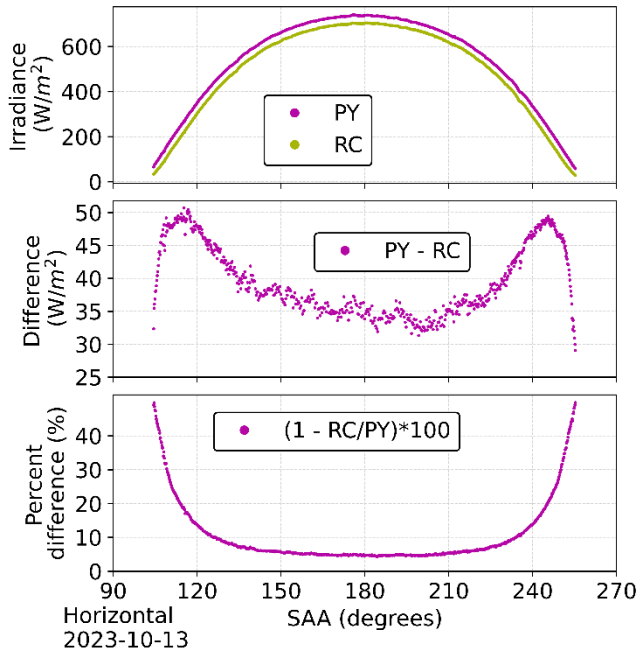

Figure 1. Reference cell and pyranometer data for a clear sky day.

At first glance it appears that there is a calibration issue between the two sensors. But it should be noted that if it was a simple calibration issue, the percent difference between the two sensors would be a constant value. Instead, the percent difference between changes drastically throughout the day, with a 5% difference at midday and a 40% difference at early morning and late afternoon.

The variation in the percent difference between the two sensors is the motivation for this work. The adjustment algorithm outlined in this paper modifies the pyranometer data such that it matches the reference cell data.

3. Pyranometer adjustment algorithm

The adjustment algorithm, relies on a reference cell model that can accurately predict the output of the reference cell from spectral data (and other inputs). The reference cell model has a tuning parameter that must be determined by comparing the modeled and measured reference cell data during a calibration period. Once the calibration period is over and the tuning parameter is known, the reference cell model can then be used. A similar process is performed for the pyranometer. Finally, the reference cell and pyranometer models are combined to generate adjustments to the pyranometer data such that it adequately mimics the reference cell.

In previous studies, [4, 5, 6, 7, 8] the output of reference cells on horizontal, fixed tilt, one- and two-axis tracking surfaces were modeled using measured spectral irradiance and the temperature of the reference cells. The results of these studies concluded that four main factors affect the reference cell model:

1. The changing spectral distribution of incoming light.
2. The angle of incidence of the incoming light.
3. Effect of transmission of light through the glazing
4. Spectral responsivity changes due to reference cell temperature changes.

The modeled reference cell output used in this study is given by Equation 1.

$$RC_{model} = \frac{1}{K_{RC}} * \left(\frac{IAM_{RC}}{K_{RC}} * \sum R_{RC\,\lambda}(T) \cdot I_{\lambda} \right) \qquad (1)$$

Where IAM_{RC} is the incident angle modifier and is the average transmission of light through the reference cell glazing The IAM is a function of the angle of the incidence of the incoming light. To obtain the angle-of-incidence function, the incident radiation is separated into the beam irradiance and diffuse irradiance components in the plane of array surface. The diffuse irradiance is further separated into circumsolar (C), dome (D), horizon (H), and ground reflected (G) components. The various diffuse components are obtained from the Perez model [9]. Lastly the Marion model [10] is applied to the various components to generate an overall IAM_{RC} term according to Equation 2.

$$IAM_{RC} = \begin{pmatrix} DNI * Cos(SZA) * 1 + \\ DfHI_C * 1 + \\ DfHI_D * IAM_D + \\ DfHI_H * IAM_H + \\ DfHI_G * IAM_G \end{pmatrix} / \; GHI \qquad (2)$$

In Equation 2 the IAM values of each term are weighted according to the irradiance of that term. The IAM of the direct and circumsolar irradiance is 1. The IAM of the diffuse dome, horizon, and ground are computed from the Marion model. Equation 2 was computed for horizontal irradiance. From Equation 2, the resulting IAM_{RC} is a measure of the fraction of light that makes it through the glass to PV surface below. The IAM does not consider any spectral effects.

In Equation 1. $R_{RC\,\lambda}(T)$ is the spectral responsivity of the reference cell, which is a function of the reference cell temperature. An adjustment to the spectral responsivity $R_{RC\,\lambda}(T)$ was determined using the Hishikawa model [11]. I_{λ} is the spectral irradiance of the incoming light.

Essentially $R_{\lambda} \cdot I_{\lambda}$ is a measure of how much short circuit current the reference cell will generate at a particular wavelength. The sum in Equation 1. adds all these individual wavelength components up to generate a total reference cell short circuit current. Reference cells only generate current inside the wavelength range of 300 to 1300 nm.

The value of K_{RC} is a scale factor needed to match the modeled data with the measured data. The value of K differs from one because the spectral responsivity (R_{λ}) is typically normalized to one. In doing this the magnitude of RC_{model} is incorrect.

The value of K_{RC} is determined by setting the modeled data equal to the measured data and solving for K_{RC}. This is done for each data point in an initial tuning data set. The median is then computed according to Equation 3.

$$K_{RC} = Median\left(\frac{IAM_{RC} * \sum R_{RC\,\lambda}(T) \cdot I_{\lambda}}{RC_{measure}} \right) \qquad (3)$$

At first glance Equations 1 and 3 appear to contain circular logic. The key is that Equation 3 is computed from a calibration data set. From this calibration data set the value of K can be determined. This value can then be used in Equation 1 and the reference cell model will have the correct magnitude. In [12] it was shown that for a variety of reference cells, under different orientations, the ratio in Equation 3 was constant under clear sky conditions to within ±3% at the 95th level of confidence. The value of K varies for different reference cells.

Applying a similar set of equations to a Class-A pyranometer results in Equations 4 and 5.

$$PY_{model} = \frac{IAM_{PY}}{K_{PY}} * \sum R_{PY\,\lambda}(T) \cdot I_{\lambda} \quad (4)$$

$$K_{PY} = Median\left(\frac{IAM_{PY} * \sum R_{PY\,\lambda}(T) \cdot I_{\lambda}}{PY_{measure}}\right) \quad (5)$$

Note that in Equations 4 and 5, the subscripts denote pyranometer values (PY). Once again, through a calibration period the value of K_{PY} can be determined according to Equation 5.

There are two key differences between the two sets of equations, the incident angle modifier and the spectral response. Class-A pyranometers are spectrally flat and have a nearly constant spectral response over a significant portion of the wavelength range. Also pyranometers are designed to have minimal directional response (IAM ≈1). Meanwhile reference cells show the spectral response of silicon-based PV and exhibit the IAM behaviors outlined by Marion. These differences are the source of discrepancy between the two data sets shown in Figure 1.

The adjustment algorithm that converts pyranometer measured data to a corresponding "reference cell like" data set is derived as follows. Multiply and divide the right side of Equation 1 by $PY_{Measure}$.

$$RC_{model} = \left(\frac{IAM_{RC}}{K_{RC}}\right)\left(\sum R_{RC\,\lambda}(T) \cdot I_{\lambda}\right)\left(\frac{PY_{Measure}}{PY_{Measure}}\right) \quad (6)$$

Determining K_{PY} from Equation 5 ensures that the measured pyranometer data matches the modeled pyranometer data for the calibration data set. Thus, the bottom $PY_{Measured}$ term can be replaced by a $PY_{Modeled}$ term.

$$RC_{model} = \left(\frac{IAM_{RC}}{K_{RC}}\right)\left(\sum R_{RC\,\lambda}(T) \cdot I_{\lambda}\right)\left(\frac{PY_{Measure}}{PY_{Model}}\right) \quad (7)$$

Equation 4 is used to replace PY_{Model}

$$RC_{model} = \left(\frac{IAM_{RC}}{K_{RC}}\right)\left(\sum R_{RC\,\lambda}(T) \cdot I_{\lambda}\right) * \left(\frac{PY_{Measure}}{\frac{IAM_{PY}}{K_{PY}} * \sum R_{PY\,\lambda}(T) \cdot I_{\lambda}}\right) \quad (8)$$

Combing similar terms and rearranging, results to a more suggestive form. Also in Equation 9, the resulting output was renamed $PY_{Adjusted}$ to denote the fact that the PY measured data has been adjusted such that it matches a reference cell data set.

$$PY_{Adj} = RC_{model} = \left(\frac{K_{PY}}{K_{RC}}\right)\left(\frac{IAM_{RC}}{IAM_{PY}}\right)\left(\frac{\sum R_{RC\,\lambda}(T) \cdot I_{\lambda}}{\sum R_{PY\,\lambda}(T) \cdot I_{\lambda}}\right) PY_{Measure} \quad (9)$$

Equation 9 contains three ratios of pyranometer to reference cell values. The first is the ratio of the corresponding K values. This is an overall scaling factor between the two data sets. The second is the ratio of the angle of incidence functions. This accounts for the directional response differences between the two instruments. The third is a ratio of the spectral response times the spectral irradiance terms. This takes into account the spectral mismatch of the two instruments. The fourth input is the measured pyranometer data. In this way, measured pyranometer data is adjusted to a data set that would have been obtained by the corresponding reference cell.

Equation 9 can be modified to compute "pyranometer-like" data from a corresponding reference cell data set, given by Equation 10.

$$RC_{Adj} = PY_{Model} = \left(\frac{K_{RC}}{K_{PY}}\right)\left(\frac{IAM_{PY}}{IAM_{RC}}\right)\left(\frac{\sum R_{PY\,\lambda}(T) \cdot I_{\lambda}}{\sum R_{RC\,\lambda}(T) \cdot I_{\lambda}}\right) RC_{Measure} \quad (10)$$

4. Explanation of terms

Measured spectra data is not commonly available on PV sites. For this reason, in an effort to make the adjustment algorithm as accessible as possible, modeled spectral data was used for this study. The modeled spectral data was generated using PVLIB's [13] spectrl2 library based off the Bird model [14, 15]. The spectrl2 clear sky model is available in the python based PVLIB package.

The modeled spectra irradiance was generated for the horizontal orientation. This is the same orientation as the reference cell and pyranometer used in this study. The modeled data is generated at varying wavelength intervals between 5 and 100 nm. A linear interpolation was performed to generate spectral irradiance values at 1 nm intervals.

The normalized spectral irradiance for two discrete minutes is shown in Figure 2 (upper). In Figure 2, both spectra were normalized to 1 at the maximum irradiance value. At 7 AM the solar zenith angle (SZA) is 81° and the spectrum is shifted to higher wavelengths as is expected. At 12 PM the solar zenith angle (SZA) was 48° for this day. Figure 2 demonstrates that the distribution of the modeled spectrum varies throughout the day.

The short circuit current spectral responsivity of the reference cell was measured at the NREL Cell Lab under a standard lamp perpendicular to the reference cell [3]. It is standard practice to normalize the spectral responsivity

to 1 at the peak response wavelength. In doing this normalization information about the scale of the spectral response is lost, which is the reason for the value of K_{RC} in Equation 9.

In the lower panel of Figure 2, the spectral response of the pyranometer and the reference cell are shown. The spectral response of the pyranometer was estimated from the manufacturer website. Clearly the pyranometer has a much greater spectral range than the reference cell.

The summation terms of R and I in Equation 9 are applied by multiplying the corresponding R values times the irradiance values. The combination of the varying spectral irradiance distribution coupled with two very different spectral response curves generates significant difference of the two sums in Equation 9.

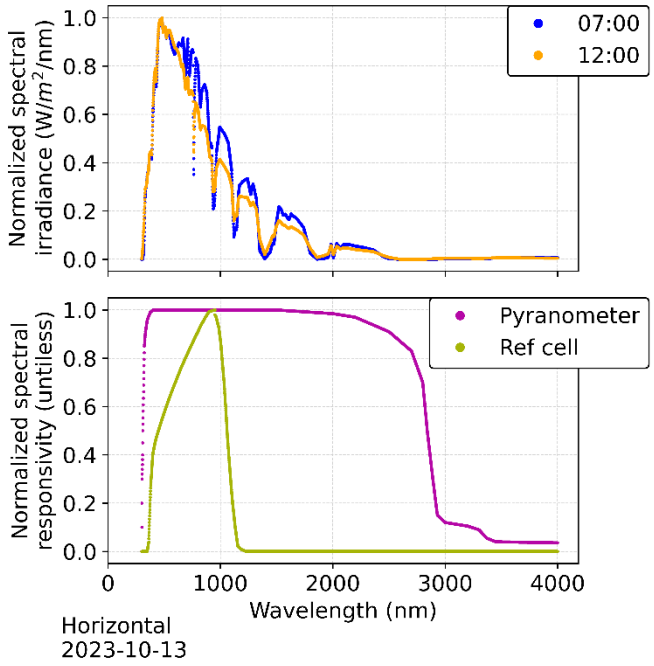

Figure 2. Modeled spectral irradiance and spectral responsivity of the pyranometer and reference cell. The spectral irradiance has been normalized to 1.

The incident angle modifier (IAM) is a measure of how much incident irradiance makes it through the glass to reach the PV surface below. Reference cells experience a IAM similar to that of PV modules. The IAM of a pyranometer is equivalent to the directional response of the sensor. The directional response of pyranometer is very close to one for all angles of incidence.

The IAM of the reference cell was computed using Equation 2. In Equation 2, the DNI data was obtained from the MIDC monitoring network. The various diffuse terms were obtained from the Perez model. Measured diffuse was one of the inputs to the Perez model. The measured diffuse was obtained from the MIDC network. The diffuse IAM components were obtained from the Marion model.

In Figure 3, the measured DNI was converted to direct horizontal irradiance (DrHI) and is plotted as the dashed orange line. The solid orange line corresponds to the DrHI after the IAM has been applied to the direct component. Figure 3 corresponds to a single clear-sky day. The horizontal axis of Figure 3 is the solar azimuthal angle.

A similar, but slightly more complicated process, was applied to the diffuse component. The measured diffuse is plotted as the dashed blue line. The diffuse was separated into the various components and the IAM was applied to each component separately. Then the IAM adjusted components were added together generating an overall IAM adjusted diffuse term, plotted as solid blue.

The global average IAM adjusted was computed by combining the direct and diffuse IAM adjusted terms. The IAM adjusted global data value is plotted as the solid purple line in Figure 3.

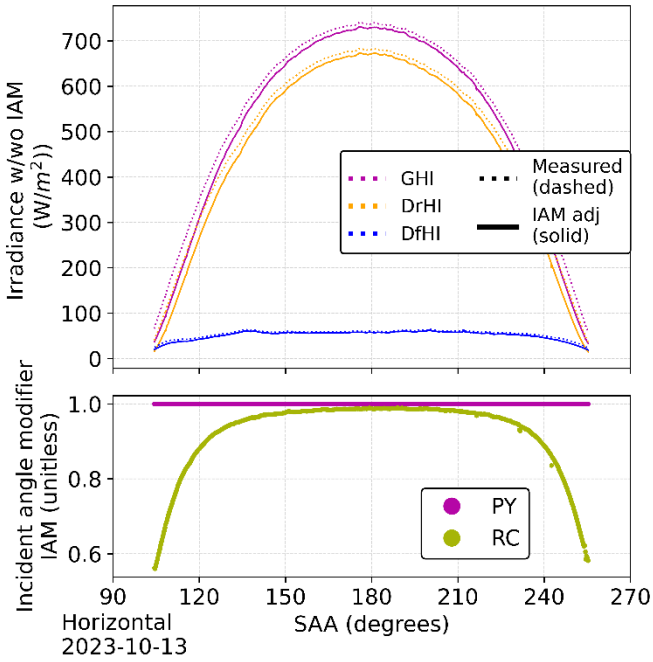

Figure 3. Incident angle modifier effects of the pyranometer and reference cell.

In the lower plot of Figure 3, the IAM of the reference cell is plotted. The IAM was computed by taking the ratio of IAM adjusted GHI irradiance relative to the unadjusted GHI irradiance. For comparison the IAM of the

pyranometer is plotted as a constant value of one of for all times of day.

5. Results

In this section the method outlined in Section 3 will be applied to the data. The methodology discussed in Section 3, required a tuning period to determine the value of K_{PY} and K_{RC}. For this study 10 days in mid-October 2023 were selected. Once the values of K are known, Equation 9 can be applied to the rest of the dataset for validation.

In Figure 4, measured reference cell data is plotted for a single clear-sky day. The numerator of the fraction in Equation 3 is also plotted. In the lower plot the value of K is plotted. K is nicely behaved throughout the day. Only at dawn and dusk does the value of K vary significantly when the irradiance is small. The trending upward line is indicative of a sensor leveling issue. The increasing value of K is still being investigated.

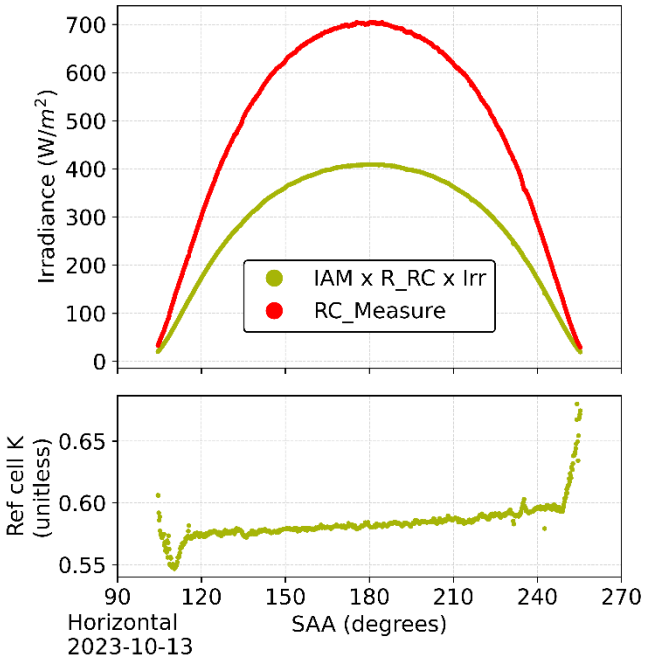

Figure 4. K_RC for a single day. The upper plot shows the inputs to Equation 3. The lower plot shows the resulting K for the entire day.

Figure 4 was for a single day. A plot of K for all clear sky data during the calibration period is shown in Figure 5.

The upper plot of Figure 5 corresponds to the value of K_{PY} for the pyranometer as computed by Equation 5 during the tuning period. The spread in the pyranometer data is attributable to the modeled spectral irradiance not being scaled correctly. The lower plot of Figure 5 shows the value of K_{RC} for the reference cell as computed by Equation 3 during the tuning period.

The modeled spectrum was computed independently of the measured global irradiance so the ±2% spread in the upper plot is to be expected. The accuracy of getting the spectral irradiance exactly correct is not critical. Because the same spectral irradiance is applied to both the spectral response of both sensors, any errors in the spectral will be applied to both sensors.

In both plots of Figure 5, the horizontal line corresponds to the median value of K for both calibration periods. These numerical values are used in Equation 9 for K_{PY} and K_{RC}.

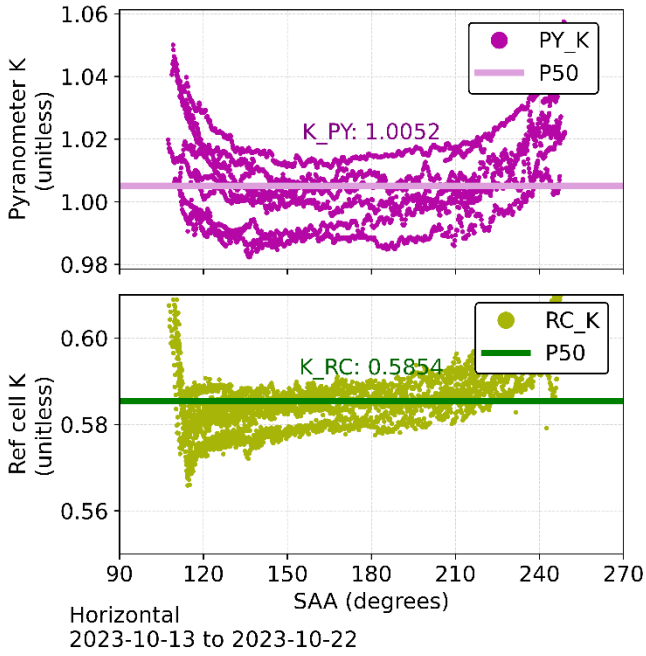

Figure 5. K_{PY} and K_{RC} for the entire calibration period. Only clear sky data is shown.

With values of K_{PY} and K_{RC}, Equation 9 can now be computed to data outside the tuning period. Figure 6 shows the pyranometer before and after the adjustment along with the corresponding reference cell data for a single clear-sky day. The adjusted pyranometer data (blue) aligns with the reference cell data (yellow) very well.

The difference between the pyranometer and reference cell is shown in the middle panel. The percent difference between the pyranometer and reference cell is shown in the lower panel. The adjusted data has minimal differences. The un-adjusted data shows the same differences that were present in Figure 1.

The results of Figure 6 are generalized to the entire test data set in Figures 7 and 8. In Figure 7, the horizontal axis is the solar azimuthal angle (SAA). In Figure 8, the

horizontal axis is the solar zenith angle (SZA). Both figures corespond to only clear sky periods. Differences in irradianc of less than 10 W/m^2 are measured for all data. For SZA values less than 70° differences of less than 2% are obtained. This 2% threshold is less than many groups use as their quality control (QC) threshold between pyarnometers. Thus the adjusted pyranometer data could be compared to reference cell data using existing QC methods.

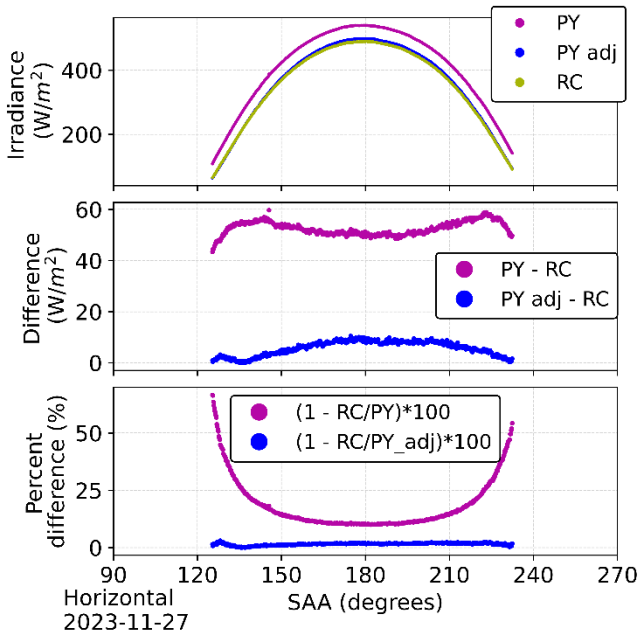

Figure 6. Adjusted pyranometer data. Comparison with reference cell data shows excellent agreement.

Similarly, reference cell data can be adjusted to match pyranometer data using Equation 10. Figure 9 shows the difference and percent difference between the adjusted reference cell data and the measured pyranometer.

The results of Figures 8 and 9 are very similar. It must be noted that the IAM calculation in Equation 9, uses some measured GHI, DNI, and DHI terms. So the results shown here are not completely independent measured pyranometer data. More work is needed to fully migrate Equation 10 over to reference cell inputs.This could be done by using decomposition models to generate DNI and DHI data from a GHI data set.

6. Conclusions

Comparing reference cell data to pyranometer data is often challenging, due to the spectral mismatch and angle of incidence variations between these technologies. Because of these differences it is difficult to compare data across technologies. Or in other words, it is difficult to compare the irradiance obtained from the short circuit current measurement of a reference cell to that of a pyranometer.

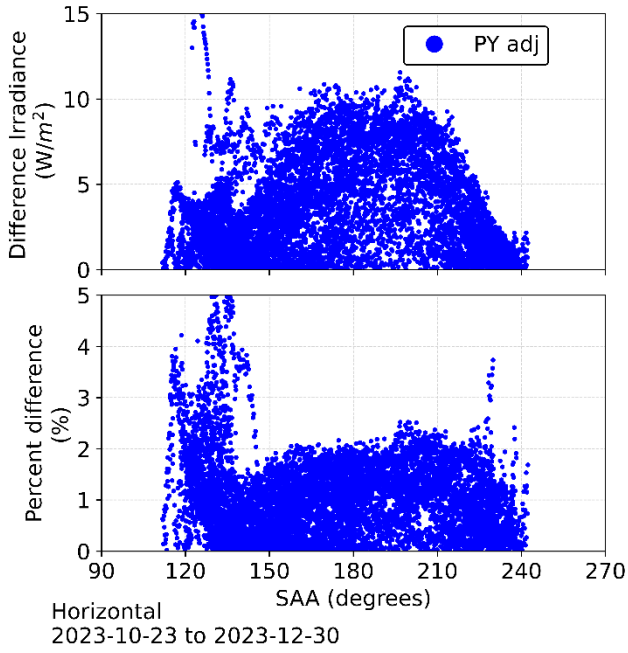

Figure 7. Adjusted pyranometer data compared to reference cell data vs solar azimuthal angle. Comparison with reference cell data shows excellent agreement.

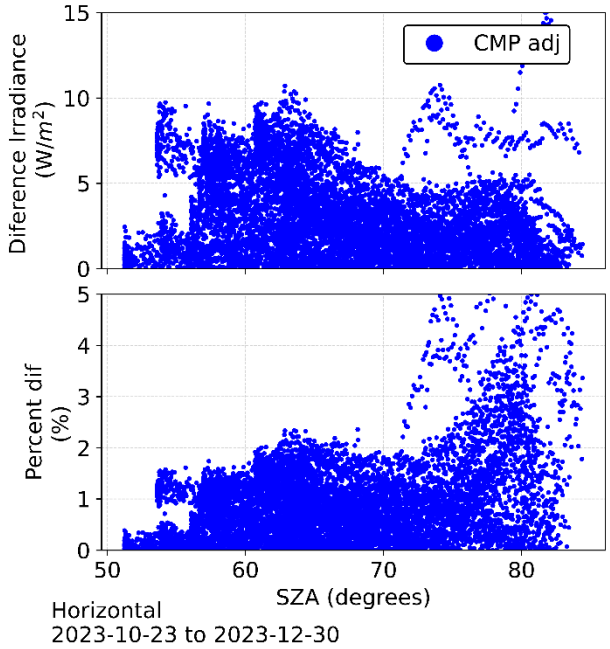

Figure 8. Adjusted pyranometer data compared to reference cell data vs zenith angle. Comparison with reference cell data shows excellent agreement with percent differences less than 2% for SZA values less than 70°.

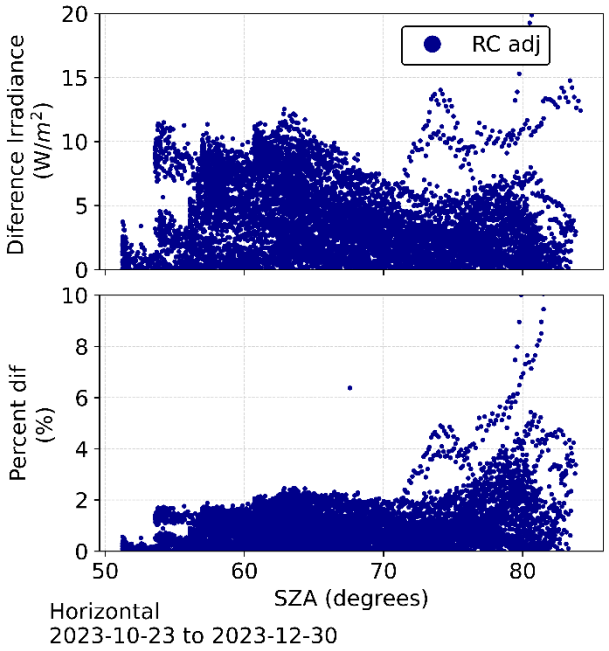

Figure 9. Adjusted reference cell data compared to pyranometer data. vs zenith angle. Comparison with reference cell data shows excellent agreement.

The adjustment method proposed here allows users to transform the results from one technology to another: Thus allowing a more true comparison.

This report has demonstrated that after the adjustment algorithm has been applied to the data, the percent difference between the two sensors was decreased to less than 2% for clear sky minutes with zenith angles less than 70°. And less than 4% over all zenith angles. The adjustment can be applied to either the pyranometer (Equation 9) or to the reference cell (Equation 10) with similar results. These differences are small enough for current QC practices to then be applied to the two data sets.

The use of modeled spectral data allows for the method to be applicable to a wide range of uses. In addition the IAM functions used in Equation 2 are easily accessible in pvlib.

More work is needed to validate and generalize the results found here. The validation steps include:

- Test the method over a longer data set.
- Test the validity the method through different seasons
- Test the method at a different locations
- Perform tests on non-clear sky days
- Test the method on other sensor orientations, two-axis tracking, one-axis tracking, and fixed tilt
- Validate that K_{RC} and K_{PY} can be determined at one site and used at another.

Future steps to generalization of the model include:

- Remove the GHI dependence on Equation 10. Currently the IAM terms used in 10 have a pyranometer dependence. If Equation 10. is to be used independent of a pyranometer, this dependence must be removed.
- Incorporate a decomposition model to obtain modeled DNI and DHI data from measured GHI data. Use these modeled DNI and DHI values in determining the IAM.
- Incorporate a spectral model that generates non-clear sky conditions.
- Account for sensors that are not perfectly leveled

This adjustment method offers users an algorithm to modify data across technologies and shows promise. Some applications such as heat calculations require broadband pyranometer data. Other applications such as PV production yield require reference cell data. Often both data types are not available at a site. This application would allow users to compute one data set from the other to fit their needs.

7. Acknowledgements

This work was sponsored by the National Renewable Energy Laboratory and the Murdoch Family Trust. Additional support for the SRML comes from the Bonneville Power Administration, and The Energy Trust of Oregon.

References

[1] A. Azouzoute, A.A. Merrouni, E.G. Bennouna, A. Ghennioui, *Accuracy Measurement of Pyranometer vs Reference cell for PV resource assessment* Energy Procedia. 157. 1202-1209. 10.1016/j.egypro.2018.11.286. , 2019

[2] Andreas, A.; Stoffel, T.; (1981). NREL Solar Radiation Research Laboratory (SRRL): Baseline Measurement System (BMS); Golden, Colorado (Data); NREL Report No. DA-5500-56488. http://dx.doi.org/10.5439/1052221

[3] M. Sengupta, et al., Solar Radiation Research Laboratory (SRRL) Final Report: Fiscal Years 2019–2021," 2022

[4] F. Vignola, et al., *Reference Cell Performance and Modeling on a One-Axis Tracking Surface* IEEE PVSC 2022

[5] F. Vignola, et al,. *Influence of Diffuse and Ground-Reflected Irradiance on the Spectral Modeling of Solar Reference Cells*, Proceedings of the American Solar Energy Society, Boulder, CO., 2021

[6] F. Vignola, et al., *Improved Field Evaluation of Reference Cell Using Spectral Measurements*, Solar Energy 215, (2021) pp. 482-491

[7] F. Vignola, et. al., *Evaluation of Reference Solar Cells on a Two-Axis Tracking Using Spectral Measurements*, SolarPACES, September 27–October 1, 2020

[8] F. Vignola et al. *Comparison of Pyranometers and Reference Cells on Fixed and One-Axis Tracking Surfaces* ASES conference precedings 2017

[9] R. Perez, et al., *Modeling daylight availability and irradiance components from direct and global irradiance*, Solar Energy 44, 271–289, 1990

[10] W. Marion, *Numerical method for angle-of-incidence correction factors for diffuse radiation incident photovoltaic modules*, Solar Energy 147 344–348, 2017

[11] Y. Hishikawa, et al., *Temperature dependence of the short circuit current and spectral responsivity of various kinds of crystalline silicon photovoltaic devices*, Japanese Journal of Applied Physics 57, 08RG17, 2018

[12] J. Peterson et al. *Modeling Reference cell performance using measured and modeled spectral data.* IEEE 2023 PVSC

[13] W. Holmgren, C. Hansen, M. Mikofski. *pvlib python: a python package for modeling solar energy systems*. Journal of Open Source Software, 3(29), 884, 2018

[14] Bird *Simple Spectral Model: spectrl2_2.c*. [https://www.nrel.gov/grid/solar-resource/spectral.html]

[15] M. Utrillas et al. *A comparative study of SPCTRAL2 and SMARTS2 parameterised models based on spectral irradiance measurements at Valencia, Spain,* Solar Energy, Volume 63, Issue 3, 1998, ISSN 0038-092X